



Cite this: DOI: 10.1039/d4sm01013b

Size dependent polarities in tribocharged dust aggregates

 Christopher Grünebeck,* Florence Chioma Onyeagusi, Jens Teiser and Gerhard Wurm 

It is long known that particles of the same material but with different sizes charge with different polarities in mutual collisions. In most cases, the smaller grains become negative. Here, we study tribocharging of (sub-)mm dust aggregates in the course of microgravity experiments by determining the charges of particles through their motion within an electric field. Similar experiments were already conducted with monolithic grains. Here, the constituent dust grains in an aggregate add complexity to the process of tribocharging in various ways. This ranges from the dust size scale, setting local surface curvatures, over shifting grains during collisions, altering the outer surfaces and potentially generating sub-surface tribocharging, to material-dependent tribocharging with a non-homogeneous dust composition. Nevertheless, in concert with the usual size dependence, the small aggregates predominantly charge negatively, the large population charges predominantly positively.

 Received 26th August 2024,
 Accepted 18th November 2024

DOI: 10.1039/d4sm01013b

rsc.li/soft-matter-journal

Introduction

Old as it might be, tribocharging is still a topic with challenging problems.¹ This might not come as a surprise as charge transfer is a complex process that depends on quite a number of parameters, from material dependence, choice of charge carriers to the influence of humidity, particle history, flexoelectrical effects and beyond.^{1–6} Our original motivation for studies in this field is planet formation. Here, charging in collisions might support the growth of larger clusters of dust aggregates in a phase where large particles are needed.^{7–9} The findings on size-dependent charging reported here might be of relevance beyond that field though.

Our work relates to a situation often encountered in tribocharging of monolithic particles of different sizes. Collisions between such particles usually end up with small grains having one polarity, large grains charging with the other polarity. In an overwhelming number of works, the small grains charge negatively.¹ Some ideas to explain this size-dependent polarities are tied to negative charge carriers, trapped electronic states or non-equilibrium surface states and the available particle surface^{10–12} Waitukaitis *et al.* also find size dependence in the usual way (small grains negative), but they argue that for this mechanism there might be too few trapped states, concluding this from thermoluminescence measurements.¹³ Besides, Toth *et al.* find small grains in a macroscopic particle sample to charge negatively but only at low humidity.¹⁴ They conclude on negative

charge carriers as well. For high humidity they postulate conductive layers on the surface. Water ions are frequently considered to be charge carriers in the first place.^{3,15} Mukherjee *et al.* suggest variations in the amount of adsorbed water as an explanation for the size dependence.¹⁶ Gu *et al.* also argue on water ions with an addition of a temperature gradient at the contact upon collision and a charge gradient going along with this.² Gallo and Lama proposed different work functions but for very small grains.¹⁷ For large grains, Liu *et al.* also suggest different effective work functions for different sizes to explain the experimental setting.¹⁸ To continue the list, Forward *et al.* find small grains to charge negatively in their studies of identical material grains.¹⁹ In another study, Forward *et al.* see a size dependence as well, using JSC (a Martian simulant) with sand sized grains.²⁰ Additionally, Bilici *et al.* find small grains to be negative and large grains to be positive in fluidized bed experiments.²¹ There seem to be fewer examples that come up with a reversed polarity (small grains are positive).²² For polymer particles, Sharmene Ali *et al.* find both cases, positive and negative small grains with large grains of the opposite polarity.²³ Also, for resin particles there are studies which show small particles to be positive.²⁴ The latter works imply that there might be a material dependence to the sign of the polarity. Electric breakdown of the environment leads to a size dependent saturation charge.²⁵ This does not seem to explain the polarity bias.⁶ However, based on the charge patch model by Grosjean *et al.*, Zhang *et al.* simulate the charging of grains in a donor–acceptor setting and find agreement to size dependent charging with positive small grains.^{6,26} How global, history preserving charging would fit into these local models for other materials has to be seen.

Lotharstrasse 1, D-47057 Duisburg, Germany.
 E-mail: christopher.gruenebeck@uni-due.de



This list is certainly far from being exhaustive. In any case, all these experiments mentioned studied macroscopic, monolithic grains. But how does a sample behave where the small and large millimeter particles are themselves aggregates of micrometer dust grains? This introduces some subtleties. It is not at all clear *a priori* if charges on different sized dust aggregates would show a polarity bias. However, if this was the case, it could constrain mechanisms for size-dependent net charge generation further. We therefore analyzed the charge on dust aggregates in microgravity experiments.

The experiment

The underlying experiment setup is shown in Fig. 1. At the drop tower in Bremen, this setup is launched within an evacuated tube, resulting in 9 s of microgravity while free-falling. Before the experiment run, the dust aggregates are placed in the particle compartment at the bottom of the experiment chamber. Still on ground, a voice coil shakes the whole chamber for 15 min at a frequency of 20 Hz with an amplitude of about 5 mm. This has been previously proven to be an efficient way to electrically charge particles through mutual collisions.⁷ During this preparation phase, the sample does not exit the particle compartment as it is held loosely in place by gravity.

Right after this initial shaking, the experiment setup is launched within the tower and microgravity sets in. Now, shaking the chamber at a decreased frequency of 8 Hz and an amplitude of 12 mm distributes the sample within the chamber volume. Qualitatively, we do not see any obvious size segregation upon release, that might have been caused by tribocharging. The aggregates are well mixed, so particles of all sizes can collide among each other. The particles are observed in front of a bright background as seen in Fig. 2.

Perpendicular to the direction of observation a well defined electric field up to 80 kV m^{-1} can be set as a high voltage is applied to two copper electrodes. Within the field, particles are accelerated toward one or the other electrode, depending on their polarity. This is shown in Fig. 2 where the right side corresponds to the direction of the positive electrode.

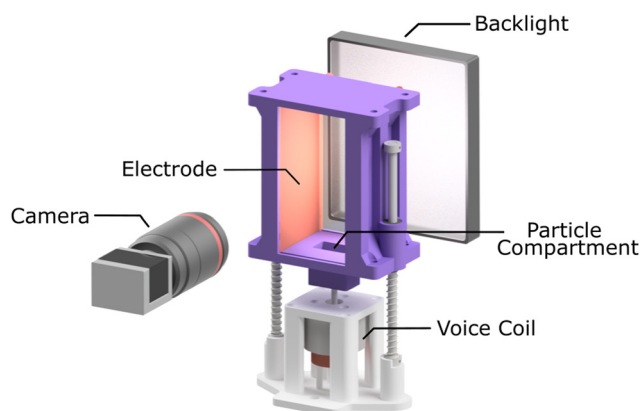


Fig. 1 Basic setup of the experiment (from ref. 27).

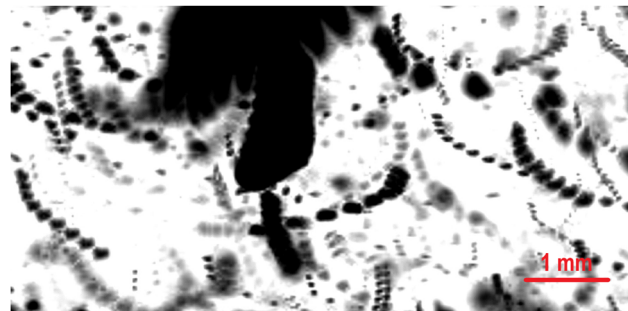


Fig. 2 Superposition of a section of experiment frames indicating aggregate trajectories as an electric field from right to left has just been turned on. Depending on their polarity, particles accelerate to one of the electrodes.

Dust sample

This work is motivated by potential astrophysical and planetary applications. As a dust sample we therefore used “Martian Global Simulant” (MGS), which is a compositional simulant of the Martian surface.²⁸ It consists of several minerals, *i.e.* plagioclase, pyroxene, olivine, magnetite, hematite, and anhydrite as crystalline and basaltic glass, hydrated silica (opal), Mg-sulfate, ferrihydrite, and Fe-carbonate in amorphous form. We further milled it down to μm -size to enable the formation of stable aggregates by surface forces. A volume size distribution of the dust grains is shown in Fig. 3.

Aggregates from this dust sample then were formed by vibrating the sample within a commercial shaker. This results in aggregates of a limited size range from around $100 \mu\text{m}$ to a few mm.

The dust sample is initially electrically conductive at a level that the grains readily discharge. No significant charge can build up during aggregate formation. Also, aggregates cannot build up internal charges due to internal conductivity. This was seen *e.g.* in experiments by Onyeagusi *et al.* where these aggregates were used without further treatment.²⁷ In contrast to these earlier studies, for this study, we heated these already formed aggregates at $120 \text{ }^\circ\text{C}$ for 48 hours the weekend before

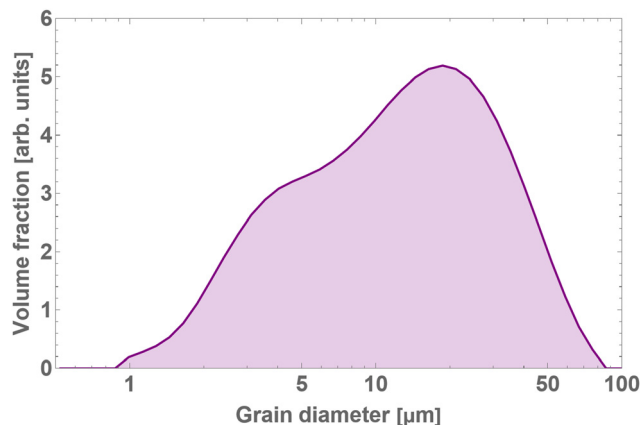


Fig. 3 Volume size distribution of the dust sample as building blocks of the aggregates.



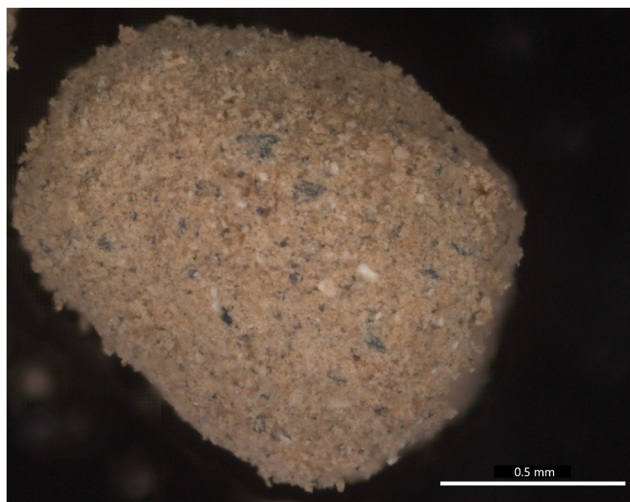


Fig. 4 Optical microscopy close-up of a dust aggregate.

the drop tower campaign. The sample then becomes electrically isolating and the aggregates become susceptible to tribocharging. We therefore consider the experiment detailed above to start with uncharged aggregates that now tribocharge if they get in contact.

Due to the choice of the material, individual dust grains do not have an identical composition. Fig. 4 shows an optical microscope image of an aggregate. This image visualizes the large number of dust grains on aggregate scale and also the inhomogeneous composition on a small scale. Individual contacts during a collision can and regularly will then be between two grains of different composition. As seen in Fig. 3, the volume fraction of the dust size peaks at about 20 μm , so that 1000 or more particles fill the volume of an aggregate. We deem the number of constituent grains to be sufficient, so that each aggregate essentially has the same average composition. Material-dependent charging should therefore average out with respect to net charging, even though there will likely be strong multipoles on the surface.

Results

Most aggregates are elongated but not extremely shaped. We therefore manually determined an average size for aggregates from the images taken during microgravity. Within the uncertainties of the third dimension, we consider this to be accurate enough in the context of this paper. We then used an aggregate density of $0.43 \text{ g cm}^{-3} \pm 0.09 \text{ g cm}^{-3}$ to calculate the aggregate mass m . This value was derived by weighing single particles and measuring their size. Important in the context of this work is the fact that the size distribution of the aggregates contains small and large aggregates. This can be seen in Fig. 5. There are way more small aggregates within the sample, but as collisions depend on cross sections, we plot the area size distribution at the bottom of this figure. At the very low end, we do have an observational bias due to the resolution of the optical system. In any case, the distribution might be split in two populations, separated by a dip at a size of about 0.4 mm.

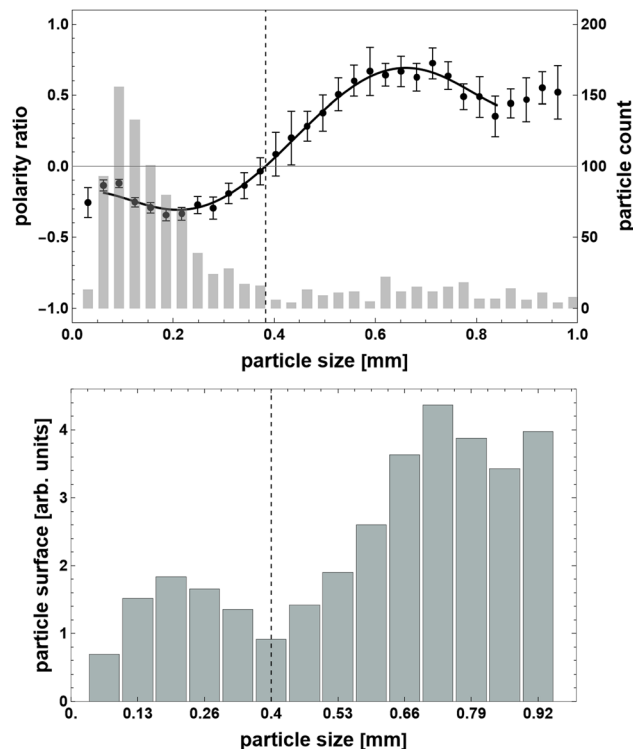


Fig. 5 Top: Running averages of the polarity of aggregates of a given size combined with the number of particles evaluated per bin; to guide the eye a polynomial approximation is overlaid on the polarity data; bottom: distribution of the total area of all aggregates of a given size. The dotted line marks the transition from negative to positive polarity.

The next important quantities are the net polarity and absolute charge of the aggregates. These can be determined from the trajectories if an electric field $E = U/d$ with voltage U and electrode distance d is applied. For the absolute charge measurement, we obtain the acceleration a through a parabolic fit of the particle motion in field direction and finally get the charge q of an aggregate as

$$q = \frac{mad}{U}. \quad (1)$$

The voltage is set to $V = 4 \text{ kV}$ while the distance between the electrodes is $d = 50.5 \text{ mm}$. Typical values for mass and acceleration are in the range of $m = 5.6 \times 10^{-6} \text{ g}$ and $a = 6.3 \times 10^{-2} \text{ m s}^{-2}$, while the uncertainties for these variables are $\Delta U = 20 \text{ V}$, $\Delta d = 0.5 \text{ mm}$, $\Delta m = 3.5 \times 10^{-6} \text{ g}$ and $\Delta a = 3.75 \times 10^{-3} \text{ m s}^{-2}$ for particles with a diameter of approximately 0.15 mm.

However, this can only be done for particles which are visible over a significant part of the trajectory. As the field of view was rather crowded (see Fig. 2) to enable high collision rates during the short microgravity time, this procedure was only done for about 30 particles. This is not enough for a detailed charge distribution. It also includes a large error for the small aggregates due to spatial resolution and attribution of a specific mass. Especially, size-dependent charge distributions are beyond this data set. Anyway, we do find values up to 1 pC



on 1 mm aggregates. This is comparable in charge density to glass beads measured in earlier works.^{29,30}

In addition to a quantitative charge measurement, we can easily attribute a polarity, depending on the electrode toward which the particles are drawn to, as the electric field is turned on. This can be done for a much larger sample of aggregates. The top of Fig. 5 shows the average polarity of a given size bin. This polarity is defined as $(N_+ - N_-)/(N_+ + N_-)$, where N is the number of positive or negative aggregates. This polarity follows the particle size, with small aggregates being predominantly charged negatively, and large ones being positive. The turning point at about 0.4 mm matches well with the transition in the size distribution of the total aggregate surface that essentially divides two different populations as seen in the bottom of Fig. 5. The polarity switch does not correspond perfectly with the size of the minimum particle area and might not be fundamental but a nice discriminator here that small aggregates charge negative and large positive. There is a small factor more area in larger (positive) grains compared to the smaller (negative) grains. However, we have a detection bias and do not see the very small grains. If they account for the difference, then the minimum would just be the average size of a particle with equal surface areas for larger particles above and smaller particles below. Then this should correspond to the size of the polarity switch, which might be the case here.

Discussion

The data very clearly show the usual trend introduced above, that is, small particles – here small aggregates – charge negatively, large ones positively. It is curious that we see such a clear size bias in polarity despite all the complexities behind dust aggregates as there are various potential add-on charge biases which might also be way more effective locally.

As a first feature, dust grains introduce their own size scale right at the surface of the dust aggregates where charge is supposed to be transferred. It will always be a contact between two (on average) equal dust grains in a collision. Local differences can therefore play no role in the large aggregate size scale. This might not be taken for granted, as *e.g.* curvature effects are considered to be important in some cases of charging.³¹ And in fact, our dust size distribution is rather wide. Forward *et al.* see a size dependence on individual grains of their fountain flow which emerge from a larger particle bed.²⁰ So there should be a local charge bias on individual dust grains which constitute the aggregates. Still, there is a mechanism which superimposes a dependence on the aggregate sizes.

Second, an aggregate is not a monomorphic structure. This is nicely visualized in Fig. 4 with fragile dust grains dangling at the side of the aggregate. “Aggregate” as a term might mean different things in different communities. At this point, we therefore need to define this somewhat better. In our studies, a dust aggregate is a collection of dust grains which only stick together by surface forces. That is, the grains are very weakly bound to each other. The individual grains are not immobile. If

two dust grains from different aggregates get into contact upon collision, the grains and their local surroundings inelastically shift within the aggregate. This is *e.g.* visible in microscopical images of two colliding dust aggregates in Jankowski *et al.*³² It is also visible in experiments by Onyeagusi *et al.*, where small parts of aggregates are shed off in collisions.³³

That the surface is unstable to small scale motions can also roughly be estimated if we compare the rebound forces in an aggregate collision with the adhesive forces between the constituent grains. Kelling *et al.* estimate the collision time between two mm dust aggregates to $\Delta t = 0.1$ ms for a $m = 10^{-7}$ kg particle.³⁴ If we approximate the rebound force by $F_r = p/\Delta t$ with momentum $p = m \cdot v$ and velocity $v = 0.1$ m s⁻¹, we get $F_r = 10^{-4}$ N. On the other side, using JKR theory, we can estimate the cohesive force by $F_c = 3/2\pi\gamma d$ with particle size d and surface energy $\gamma = 0.07$ J m⁻².^{35,36} Particle size here refers to the dust grains as they are in contact. If we assume $d = 1$ μm we get $F_c = 10^{-7}$ N. This is 3 orders of magnitude less than the rebound force. While the forces might mostly be balanced by force chains with details beyond this work, it is easy to shift grains on the surface. This is in line with small parts of the surface being shed off as mentioned above.³³

Due to high coefficients of restitution in collisions with aggregates composed of small grains, not the whole aggregate will be influenced in a single collision, as this would require more energy.³⁷ In fact, this essentially elastic nature of the dust aggregates gave such collisions the name bouncing barrier in planetesimal formation.³⁸ Forces on surface grains act on both collision partners. So they are independent of the aggregate size and also shifts of grains within an aggregate occur for small and large aggregates, though in detail, force chains in very small aggregates might add some modification. In any case, there will be shifting of grains close to the surface.

This might have two effects.

On one side, it alters the outer surface of the aggregate, burying some surface that is no longer available in the next collision but displaying some new surface from within the aggregate. That efficiently increases the active surface available for collisions. Or in other words, efficient recycling would erase the history of the surface charging and therefore decrease any effects that might arise from the difference in the absolute amount of surface of small and large particles. We cannot quantify this effect for the given sample, but would speculate that this makes it less likely that contacting different amounts of surfaces on small and large aggregates would be the main parameter for size-dependent charging.

On the other side, as grains shift within an aggregate, there will also be an additional triboelectric charge separation within an aggregate, somewhat below the surface. This charge might find its way to the outer surface during collisional evolution, turning the internal charge inside out and *vice versa*. This would then be a different, pre-charged surface. Some internal charges will also prevail. This internal charging is a process that we only postulate here and which can currently not be analyzed. This would make the situation very complex, however, as any surface charge added would obviously not impact any process that leads to the size-biased net charge.



As a rather extreme manifestation of this process, highly charged dust grains or very small clusters might be separated upon collisions. Also, depending on the presence of a local electric field caused by the other aggregate, (charged) dust grains might move from one aggregate to the other.^{27,32,39}

Finally, Forward *et al.* used a multi-mineral planetary surface simulant, just as we do here.²⁰ For aggregates, the mean dust composition, averaging over thousands of constituent grains, is still the same as outlined above. This might qualify for “same material” charging. However, individual contacts will be between quite different minerals most of the time. Therefore, there will also be a local material related charge bias. Again, the aggregate size-dependent charge mechanism is obviously superimposing this.

All these mobility and variety aspects of dust grains as basic aggregate units suggest that the size bias is not an intrinsic feature of the surface contacts. We might directly rule out models that depend on the amount of adsorbed water as our samples were preheated. Trapped electron states were ruled out before. Models that rely on patches on certain materials might be hard to reconcile with the material variety and the bias included in our experiments, though this is not a hard rule out. In addition though, any model depending on the total surface area is challenged by the mobility of dust grains and effectively larger area of the aggregates going along with this. This essentially makes all effective surfaces large. Also, (effective) work functions are likely not relevant in our aggregates setting with individual grains being the same in small and large aggregates. Overall, we would therefore argue that size-dependent charging needs to rely on a global, size-dependent mechanism. The different current models seem to be inappropriate to our situation. So we leave our findings here as another finding of size dependent polarity but for a complex case.

Conclusion

Colliding dust aggregates charge each other *via* tribocharging. We measured this by observing particle motion within a capacitor under microgravity conditions. There are two different size scales – the aggregate size and the composing dust grain size. However, there is a clear correlation between the polarity of the charge and the overall aggregate size. Following the literature trend, small aggregates charge negatively, larger ones positively. This implies that the individual dust grain properties and surface contact charging are not the driver of size-dependent polarities, but there is presumably a mechanism missing that is superimposing local charging.

Data availability

The raw data are part of a larger data set used for a variety of further evaluations and are currently not publicly available. All significant data deduced for the purpose of this paper are part of the figures and text constituting this paper.

Conflicts of interest

There are no conflicts to declare.

Acknowledgements

This project is supported by DLR Space Administration with funds provided by the Federal Ministry for Economic Affairs and Climate Action (BMWK) under grant number 50 WM 2142, 50 WM 2442, and 50 WK 2270C. We also appreciate the constructive comments by the three anonymous reviewers.

Notes and references

- 1 D. J. Lacks and T. Shinbrot, *Nat. Rev. Chem.*, 2019, **3**, 465–476.
- 2 Z. Gu, W. Wei, J. Su and Y. C. Wah, *Sci. Rep.*, 2013, **3**, 1337.
- 3 V. Lee, N. M. James, S. R. Waitukaitis and H. M. Jaeger, *Phys. Rev. Mater.*, 2018, **2**, 035602.
- 4 G. Grosjean and S. Waitukaitis, *Phys. Rev. Lett.*, 2023, **130**, 098202.
- 5 C. A. Mizzi and L. D. Marks, *Nano Lett.*, 2022, **22**, 3939–3945.
- 6 Y. Zhang, A. Ozel and C. M. Hartzell, *Powder Technol.*, 2024, **431**, 119029.
- 7 T. Steinpilz, K. Joeris, F. Jungmann, D. Wolf, L. Brendel, J. Teiser, T. Shinbrot and G. Wurm, *Nat. Phys.*, 2020, **16**, 225–229.
- 8 J. Teiser, M. Kruss, F. Jungmann and G. Wurm, *Astrophys. J.*, 2021, **908**, L22.
- 9 G. Wurm and J. Teiser, *Nat. Rev. Phys.*, 2021, **3**, 405–421.
- 10 J. Lowell and W. S. Truscott, *J. Phys. D: Appl. Phys.*, 1986, **19**, 1273.
- 11 D. J. Lacks, N. Duff and S. K. Kumar, *Phys. Rev. Lett.*, 2008, **100**, 188305.
- 12 N. Duff and D. J. Lacks, *J. Electrostat.*, 2008, **66**, 51–57.
- 13 S. R. Waitukaitis, V. Lee, J. M. Pierson, S. L. Forman and H. M. Jaeger, *Phys. Rev. Lett.*, 2014, **112**, 218001.
- 14 J. R. I. Toth, A. K. Phillips, S. Rajupet, R. M. Sankaran and D. J. Lacks, *Ind. Eng. Chem. Res.*, 2017, **56**, 9839–9845.
- 15 F. Jungmann, F. C. Onyeagusi, J. Teiser and G. Wurm, *J. Electrostat.*, 2022, **117**, 103705.
- 16 R. Mukherjee, V. Gupta, S. Naik, S. Sarkar, V. Sharma, P. Peri and B. Chaudhuri, *Asian J. Pharm. Sci.*, 2016, **11**, 603–617.
- 17 C. Gallo and W. Lama, *IEEE Trans. Ind. Appl.*, 1976, **IA-12**, 7–11.
- 18 X. Liu, J. Kolehmainen, I. Nwogbaga, A. Ozel and S. Sundaresan, *Powder Technol.*, 2020, **375**, 199–209.
- 19 K. M. Forward, D. J. Lacks and R. M. Sankaran, *Phys. Rev. Lett.*, 2009, **102**, 028001.
- 20 K. M. Forward, D. J. Lacks and R. M. Sankaran, *Geophys. Res. Lett.*, 2009, **36**, L13201.
- 21 M. A. Bilici, J. R. Toth, R. M. Sankaran and D. J. Lacks, *Rev. Sci. Instrum.*, 2014, **85**, 103903.
- 22 D. Carter and C. Hartzell, *J. Electrostat.*, 2020, **107**, 103475.



- 23 F. Sharmene Ali, M. Adnan Ali, R. Ayesha Ali and I. I. Inculet, *J. Electrostat.*, 1998, **45**, 139–155.
- 24 A. Sowinski, L. Miller and P. Mehrani, *Chem. Eng. Sci.*, 2010, **65**, 2771–2781.
- 25 R. D. Cruise, K. Hadler, S. O. Starr and J. J. Cilliers, *J. Phys. D: Appl. Phys.*, 2022, **55**, 185306.
- 26 G. Grosjean, S. Wald, J. C. Sobarzo and S. Waitukaitis, *Phys. Rev. Mater.*, 2020, **4**, 082602.
- 27 F. C. Onyeagusi, J. Teiser, T. Becker and G. Wurm, *Mon. Not. R. Astron. Soc.*, 2024, **529**, 1989–1994.
- 28 K. M. Cannon, D. T. Britt, T. M. Smith, R. F. Fritsche and D. Batcheldor, *Icarus*, 2019, **317**, 470–478.
- 29 T. Steinpilz, J. Teiser and G. Wurm, *Astrophys. J.*, 2019, **874**, 60.
- 30 F. Jungmann, M. Kruss, J. Teiser and G. Wurm, *Icarus*, 2022, **373**, 114766.
- 31 G. J. Turner and C. D. Stow, *J. Geophys. Res.: Atmos.*, 2022, **127**, e2021JD035552.
- 32 T. Jankowski, G. Wurm, T. Kelling, J. Teiser, W. Sabolo, P. J. Gutiérrez and I. Bertini, *Astron. Astrophys.*, 2012, **542**, A80.
- 33 F. C. Onyeagusi, C. Meyer, J. Teiser, T. Becker and G. Wurm, *Atmosphere*, 2023, **14**, 1065.
- 34 T. Kelling, G. Wurm and M. Köster, *Astrophys. J.*, 2014, **783**, 111.
- 35 K. L. Johnson, K. Kendall and A. D. Roberts, *Proc. R. Soc. London, Ser. A*, 1971, **324**, 301–313.
- 36 T. Bogdan, C. Pillich, J. Landers, H. Wende and G. Wurm, *Astron. Astrophys.*, 2020, **638**, A151.
- 37 K. Joeris, L. Schönau, M. Keulen, P. Born and J. E. Kollmer, *npj Microgravity*, 2022, **8**, 36.
- 38 A. Zsom, C. W. Ormel, C. Güttler, J. Blum and C. P. Dullemond, *Astron. Astrophys.*, 2010, **513**, A57.
- 39 F. C. Onyeagusi, F. Jungmann, J. Teiser and G. Wurm, *Planet. Sci. J.*, 2023, **4**, 13.

